This is the author accepted manuscript.
Accepted on 27 June 2023 for publication in Journal of Engineering in Medicine.
https://uk.sagepub.com/en-gb/eur/journal/proceedings-institution-mechanical-engineers-part-h-journal-engineering-medicine

Mechanical Influence of Tissue Scaffolding Design with Different Geometries using Finite Element Study

Xinyi An[1], Perk Lin Chong[1], Iman Zohourkari[2], Sandipan Roy[3], Ali Merdji[4], Constance Linda Gnanasagaran[5], Foad Faraji[1,] Lip Kean Moey[6]
Mohammad Hossein Yazdi[7]
[1]School of Computing, Engineering and Digital Technologies, Teesside University, Middlesbrough TS1 3BX, United Kingdom.
[2]Department of Mechanical Engineering, Birjand University of Technology, Birjand, Iran.
[3]Department of Mechanical Engineering, SRM Institute of Science and Technology, Kattankulathur, Chennai 603203, India.
[4]Faculty of Science and Technology, Department of Mechanical Engineering, University of Mascara, Algeria.
[5]Department of Mechanical Engineering, Kingston University, Roehampton Vale Campus, London, SW15 3DW, United Kingdom
[6]Center for Modelling and Simulation, Faculty of Engineering, Built Environment & Information Technology, SEGi, 47810, Selangor, Malaysia.
[7]New Materials Technology and Processing Research Center, Department of Mechanical Engineering, Neyshabur Branch, Islamic Azad University, Neyshabur, Iran.

Abstract

The mechanical properties of tissue scaffolds are essential in providing stability for tissue repair and growth. Thus, the ability of scaffolds to withstand specific loads is crucial for scaffold design. Most research on scaffold pores focuses on grids with pore size and gradient structure, and many research models are based on scaffolding with vertically arranged holes. However, little attention is paid to the influence of the distribution of holes on the mechanical properties of the scaffold. To address this gap, this research investigates the effect of pore distribution on the mechanical properties of tissue scaffolds. The study involves four types of scaffold designs with regular and staggered pore arrangements and porosity ranging from 30% to 80%. Finite element analysis (FEA) was used to compare the mechanical properties of different scaffold designs, with von-Mises stress distribution maps generated for each scaffold. The results show that scaffolds with regular vertical holes exhibit a more uniform stress distribution and better mechanical performance than those with irregular holes. In

contrast, the scaffold with a staggered arrangement of holes had a higher probability of stress concentration. The study emphasized the importance of balancing porosity and strength in scaffold design.

Keywords: Mechanical Influence, Tissue Scaffolding, Different Geometries, Pore distribution, FEA

1. Introduction

Bone remodelling is an essential process for human growth and development and the bone damage is a cause of bone remodelling. However, if the lost or damaged bone area is large, the bone cannot heal through its remodeling process [1]. In the repair of tissues or organs, tissue transplantation and allogeneic tissue replacement have certain limitations. The emergence of tissue engineering (TE) has solved this problem. Tissue scaffolding provides not only mechanical functions for damaged parts but also accelerates tissue repair by incorporating biological factors that can be used to stimulate tissue repair to the scaffold [2]. Bone tissue engineering scaffolds also have individual requirements as a substitute for modern biological bone. Excellent scaffolding should strike a balance between biocompatibility and mechanical properties [3]. Scaffolding needs to be biocompatible, biodegradable, and will not produce harmful substances to disrupt the environmental balance in the body. While being highly porous, the mechanical properties of its structure should also be excellent, with a certain degree of toughness and load-bearing capacity, providing a particular automated environment for tissue repair [4].

Metals have been studied as materials for tissue scaffolding due to their promising mechanical properties and biocompatibility. These materials exhibit physical properties, such as Young's modulus, that closely resemble those of bones, but surpass bones in terms of structural strength and stability [5]. Among them, Titanium, as one of the biocompatible elements, is a promising material for implants and compared to solid ones, porous structures offer several advantages. As an example, implants with porous materials show improved bone ingrowth [6-7]. The range of Young's modulus of human

bone tissue is about 4-30 GPa [8]. Due to the risk of stress shielding, it is crucial to ensure that the Young's modulus of the scaffold matches that of the surrounding tissues. Titanium alloy is an optimal choice as it has a lower Young's modulus than traditional alloys, allowing for a closer match to the natural bone structure. Additionally, this material offers excellent corrosion resistance, making it an attractive option for medical applications [9]. A porous titanium scaffold shows a good match with bone tissue. It can promote the growth and differentiation of cells on the scaffold [10], and by adjusting the porosity in the structure of a titanium scaffold, it can have more suitable mechanical properties for implantation in the human body [11].

The emergence of computer-aided tissue engineering (CATE) has become an indispensable field in tissue engineering [12]. Among various analysis methods, finite element analysis (FEA) is an effective method in modelling mechanical responses of a scaffold structure. Most studies have shown that the mechanical performance results simulated by FEA are basically consistent with the actual compression test results [13-14], which significantly reduce the cost of experiments for evaluating performance of custom scaffolds [15]. Numerical simulations are mainly used to obtain the apparent Young’s modulus and to check the strength of tissue scaffolds. These two mechanical properties are related to whether the scaffold can have a certain support ability in the body or not [16]. To prevent stress shielding [17], whether tissue engineering scaffolding can simulate the mechanical properties of human bone is a crucial concern [18]. Titanium alloy as the material and modelled as Schwarz's minimal surface based on the ISM method. The finite element results show that the stiffness of the scaffold model obtained by parameterization meets the stiffness range of human cortical bone [19]. As a functionally graded structure of bone, its mechanical strength will change with the arrangement. The emergence of functionally graded scaffolding (FGS) is to simulate the changing structure of natural bones designed a three-layer gradient lattice based on FGS to achieve functional gradient by changing the thickness of the support rod [20-21]. Compared with a uniform crystal lattice, the design of a graded crystal lattice can meet the different requirements for mechanical properties of different parts.

Different from network structure, it has proved that a gradual lattice scaffold based on the sheet structure has better absorption capacity and stable growth of absorption efficiency and moreover, shows a better mechanical property [22]. In addition, to satisfy the mechanical properties similar to those of natural bone, the biocompatibility of the scaffold must also be satisfied. The proliferation and growth of osteoblasts as an example to study the biological activity of functionally graded titanium alloy structures. The results show that this structure is conducive to cell adhesion and proliferation [23]. In vitro cell tests conducted on scaffolds that meet the range of mechanical properties of human bones. They also used Ti6Al4V as the material to design three scaffolds that change the strut orientations to change the structure. In vitro tests show that human osteoblasts have a strong ability to synthesize on this titanium scaffold [24]. Compared to untreated scaffolds with mechanical properties similar to human cancellous bone, the biological activity of porous titanium scaffolds that have undergone chemical treatment and heat treatment has been significantly improved [25].

For the design of the pores of tissue scaffolds, most of the scaffolds as mentioned above consider the design factors of the scaffold pore size or gradient pores, and the arrangement of the holes is usually orderly. The purpose of this research is to explore the influence of pore distribution on the mechanical properties of scaffolding. Four design types of scaffolds were considered. Finite element analysis (FEA) was used to compare the apparent Young's modulus of different design types with regularly arranged pores and staggered pores. Besides, to predict the influence of porosity on various design parameters, the scaffold porosity range of 30% to 80% were studied.

2. Methodology

2.1 Design Porous Scaffolding

The Siemens NX software is used to produce 3D models of scaffolds. Through the standard Boolean process, the pore structure is superimposed on the cube and the cylinder. The superimposed pore structure is circularand square, thus eight different designs of scaffolds were created as shown in Figure 1. Changing the shape of the basic

unit block of the scaffold and its porosity and hole arrangement are the main design methods. The cubic scaffold is in 10 mm × 10 mm × 10 mm, where the cylindrical scaffold is in 10mm diameter and 10 mm height. Cylindrical structures A and B display regular square and circular porous arrangements measuring 0.98mm × 0.98 mm and 1.1 mm in diameter, respectively, while structures A' and B' exhibit the same patterns but in a staggered arrangement. Cubic structures C and D also show regular square and circular porous arrangements of the same dimensions, with staggered arrangements present in structures C' and D'.

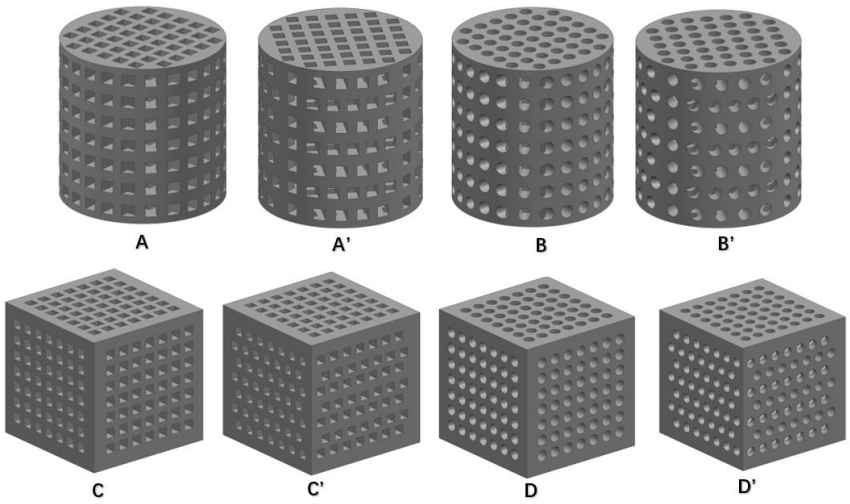

Figure 1: Porous Scaffolds (A) Cylindrical with regular square porous arrangement (A') Cylindrical with staggered square porous arrangement (B) Cylindrical with regular circular porous arrangement (B') Cylindrical with staggered circular porous arrangement (C) Cubic with regular square porous arrangement (C') Cylindrical with staggered square porous arrangement (D) Cylindrical with regular circular porous arrangement (D') Cylindrical with staggered circular porous arrangement

The apparent Young's modulus of natural bones decreases with porosity increasing. To satisfy mechanical properties and biological activity, the porosity is usually set in the range of 66% to 88% [26]. In this study, the porosity used was 30 to 80% to investigate the influence of the pore distribution on the mechanical properties of the scaffold and explore the range of porosity in which the titanium scaffold meets the range of apparent Young's modulus of human bone.

The porosity is the percentage of the pore volume to the original total volume of the material without openings. Know the volume of the designed unit porous model through the software. The porosity of the designed tissue engineering scaffold is defined according to the following formula

$$P = \left(1 - \frac{V_{Rem}}{V}\right) \times 100\% \quad (1)$$

Where V_{Rem} is the volume of the cell porous model and V is the original volume of the model.

The number of holes for each designed scaffold and the position of the holes on the scaffold are the same. The porosity here is mainly obtained by controlling the size of the holes. By keeping Constant the pore size and changing numbers and their distribution, different porosities can be obtained. However, to obtain a scaffold with a specific porosity, due to the change in porosity, the distribution and number of pores on the scaffold will also change, which may result in very different internal structures with different porosities. The internal structure may also affect the mechanical properties of the scaffold. Therefore, to avoid this situation, the size of the pores has been changed to obtain different porosities.

2.2 Finite element analysis (FEA)

Siemens NX12 was used for the finite element models to predict the mechanical responses of different designs of tissue scaffolds and evaluate the influence of porosity on the apparent Young's modulus of scaffolds. The material used for numerical analysis is titanium alloy (Ti6Al4V) which is an excellent bone substitute material. Its material properties are assigned as Young's modulus E=110 GPa and Poisson's ratio v=0.3.

To balance the accuracy of the FE model and the calculation time, the sensitivity of the mesh was analyzed, Figure 2 shows the Convergence graph of a cubic scaffold with a 50% porosity square hole. Considering the geometric intricacies, the use of a hexagonal mesh may lead to distorted meshes. Thus, for accurately capturing the significant

variations in porosity, it is more practical to use a 3D tetrahedron elements despite the overall simplicity of the geometry. Additionally, to ensure the reliability of the obtained results, a mesh convergence study has been conducted as shown in Figure 2. Based on the convergence study the grid size of 0.7mm is selected and respective number of elements is 60345 as shown in Figure 3.

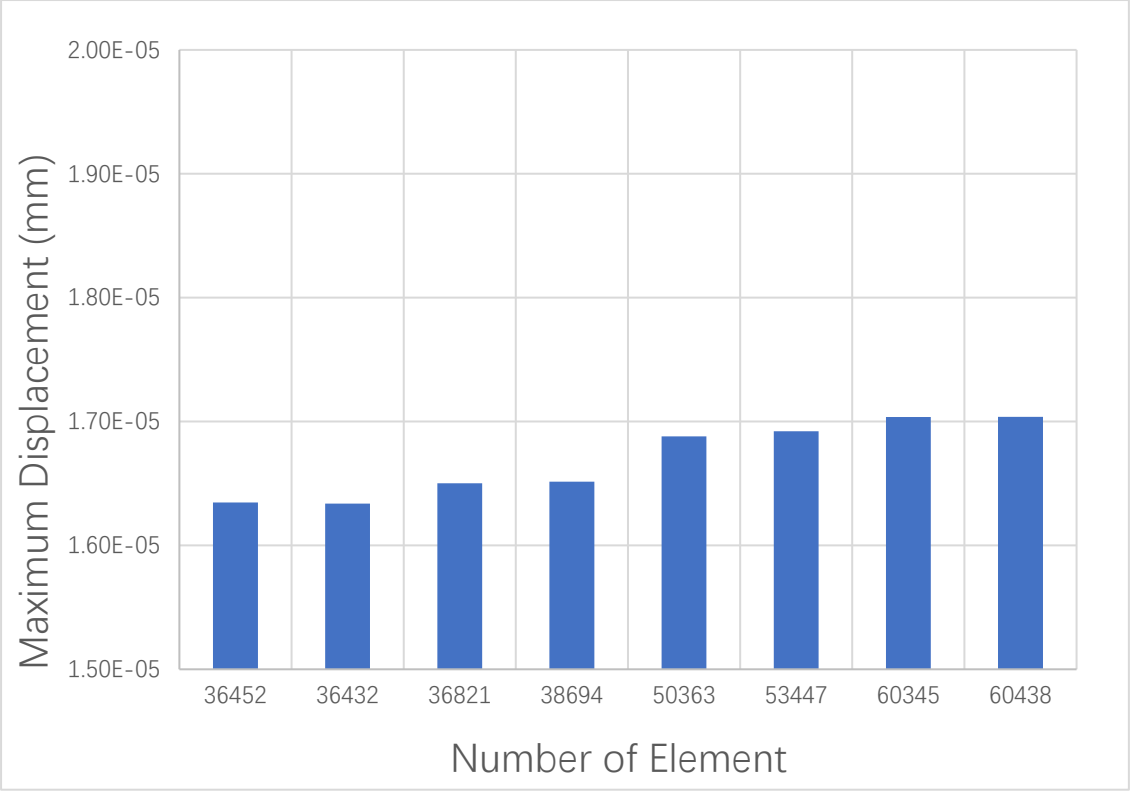

Figure 2: Convergence of Maximum Displacement with Respect to Number of Element

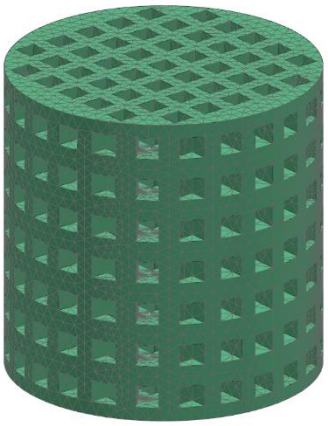

Figure 3: 3D Model with 0.7mm mesh size

The boundary conditions used to evaluate the mechanical performance of the scaffold are shown in the Figure 4. A simulated axial compression test was carried out on the model. A force was applied to face block A in axial direction, and constraints were added to the opposite face of the scaffold to prevent its displacement. The total axial force applied to the shown surface is equal to 5N.

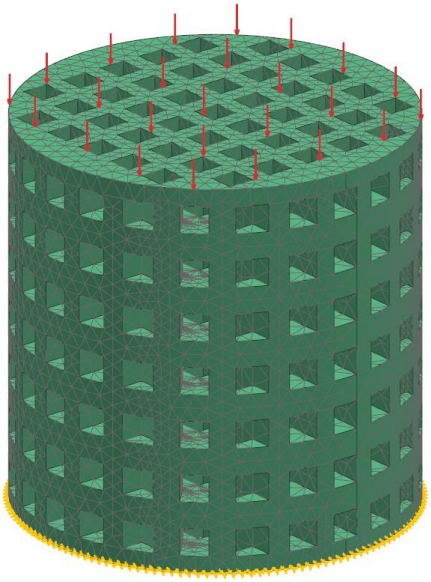

Figure 4: Boundary condition and load applied to the scaffold

Considering the load amount and displacement results obtained by FEA simulation, the apparent Young's modulus of scaffolds with different porosities were calculated by

applying formula (2). Since the apparent Young's modulus of the scaffold under a specified porosity is constant, it can be seen from the formula that the magnitude of the applied load will not affect the apparent Young's modulus of the scaffold, so for easy calculation, the force applied here is 5N.

$$E_S = \frac{FL}{A\Delta L} \tag{2}$$

Where F is the applied load, L is the initial length of the model, A is the initial cross-sectional area, and ΔL is the displacement of the support after the load is applied.

3. Results and discussion

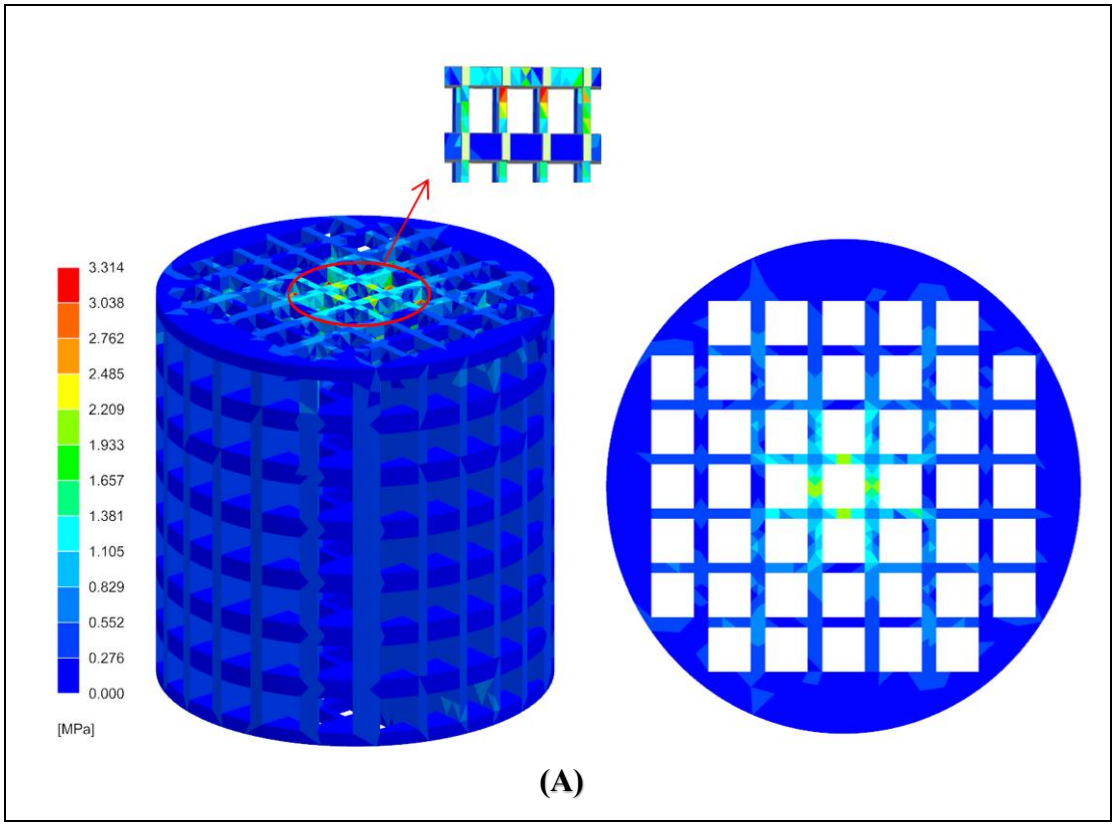

(A)

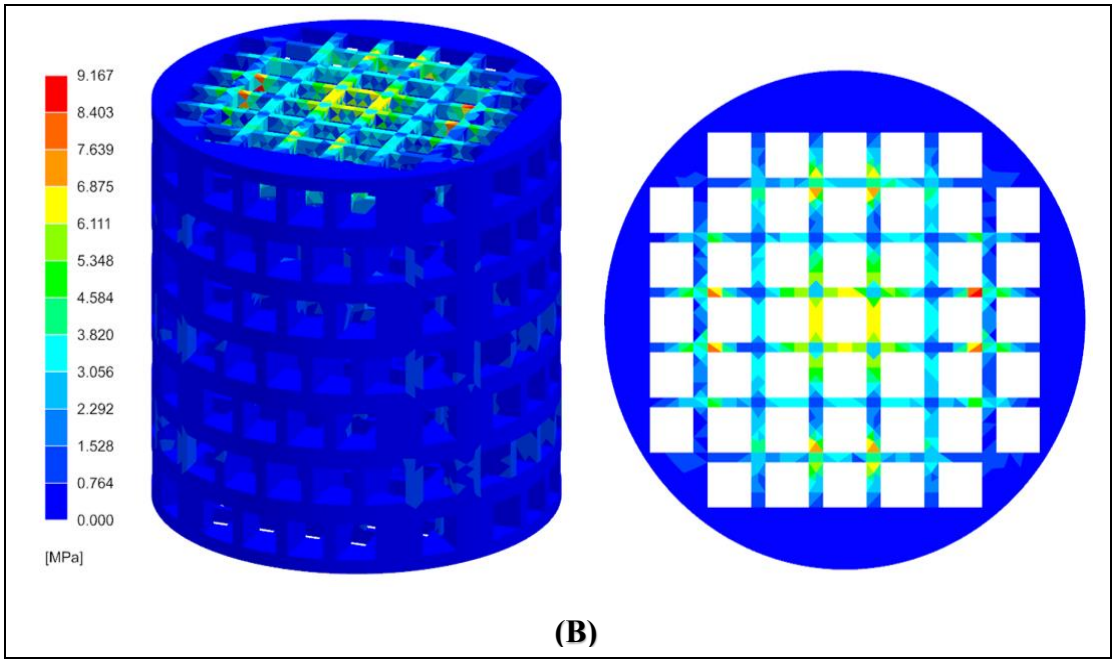

Figure 5: von Mises stress distribution of cylindrical scaffold with square hole.

Finite element models for eight types of scaffolds with regular and irregular holes were developed and their mechanical properties were calculated. Figure 5 shows the von Mises stress distribution of a scaffold with a cylindrical basic unit shape. For tissue engineering scaffolds, it is generally believed that scaffolds with high porosity can better promote cell aggregation and blood vessel formation. However, too high porosity will reduce the mechanical strength of the scaffold [27]. Therefore, it is very important to make a balance between porosity and strength of a scaffold. So, von Mises stress distribution map of the scaffold with a porosity of 70% is selected here.

As shown in Figure 5 (A), the maximum stress of a scaffold with vertically ordered holes mainly occurs at the pillar below the loading surface. The maximum stress of the scaffold with staggered holes in Figure 5 (B) is concentrated on the round surface. The stress of the scaffolds of both designs can be seen on the surface where the load is applied. Compared with the regularly arranged square-hole scaffold (Figure 5A), the stress of the staggered-hole scaffold B is more widely distributed on the circular surface, and the maximum stress is on the loading surface. In a recent study, similar stress

distribution was obtained where the stress was highest on loading surface [28]. Its stress concentration distribution is regular, symmetrical up and down, and mainly distributed on the pillars far from the center of the cross section. The maximum stress of A is smaller than that of B, which is about one-third.

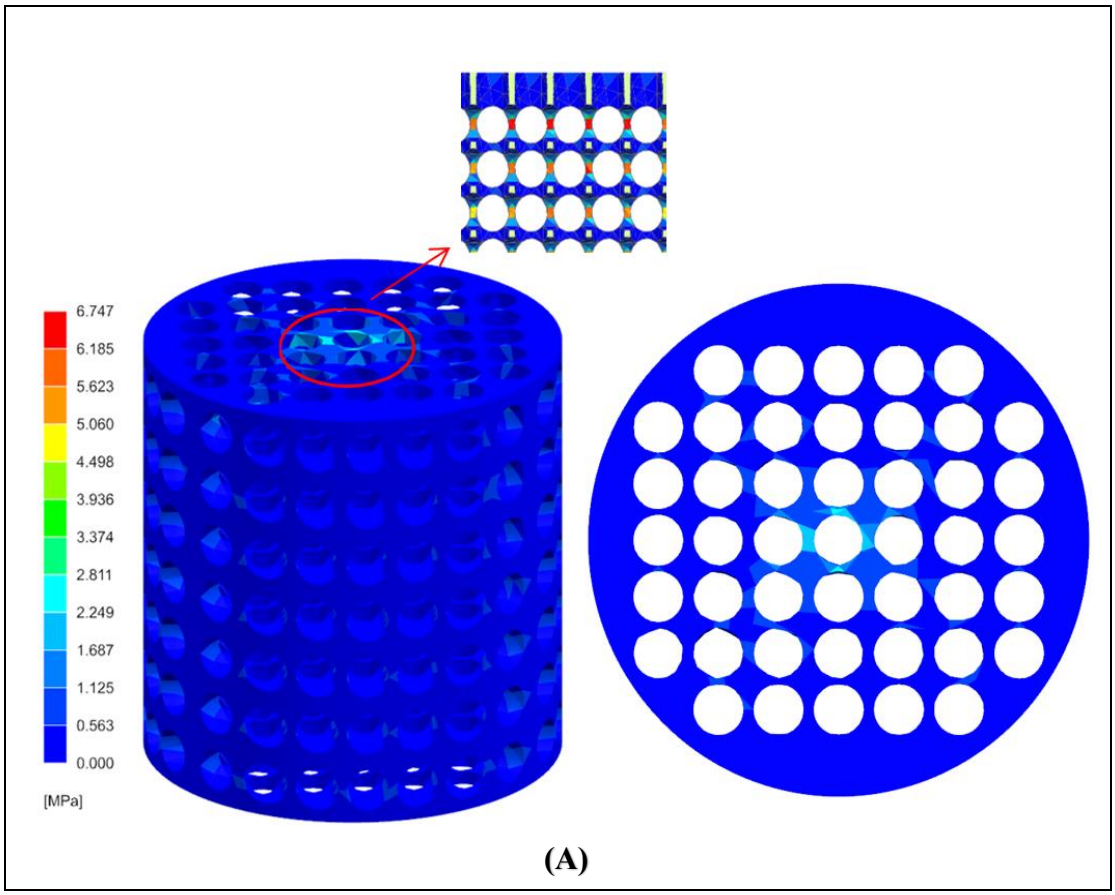

(A)

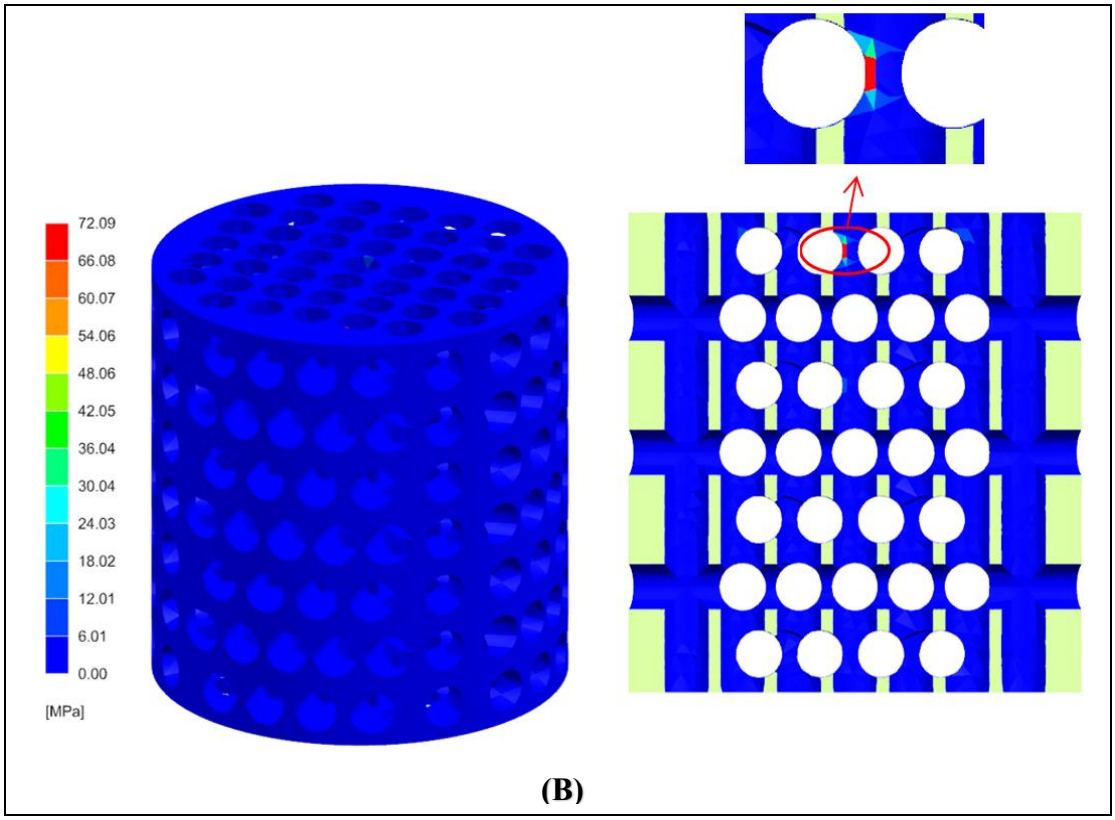

Figure 6: von Mises stress distribution of cylindrical scaffold with round hole

As for the stress distribution of the scaffold with round hole type, as shown in Figure 6, different behaviours are observed, and their stress is almost not distributed on the round surface. The stresses in Figure 6 (A) and (B) are mainly concentrated on the central pillar inside the scaffold and closest to the loading surface. The farther away from the centre of the loading surface, the smaller the stress of the A scaffold. The stress concentration of the staggered round-hole scaffold (B) is mainly concentrated on the pillars near the centre of the circle. And its maximum stress value is the largest among all scaffolds designed, as high as 72.09 MPa, which is about 11 times that of regularly arranged scaffolds. In all cylindrical scaffolding, the maximum stress of a scaffold with regular vertical holes is smaller than that of a scaffold with irregular holes. Among the four models, the lowest maximum stress Figure 5(A) is 3.314 MPa.

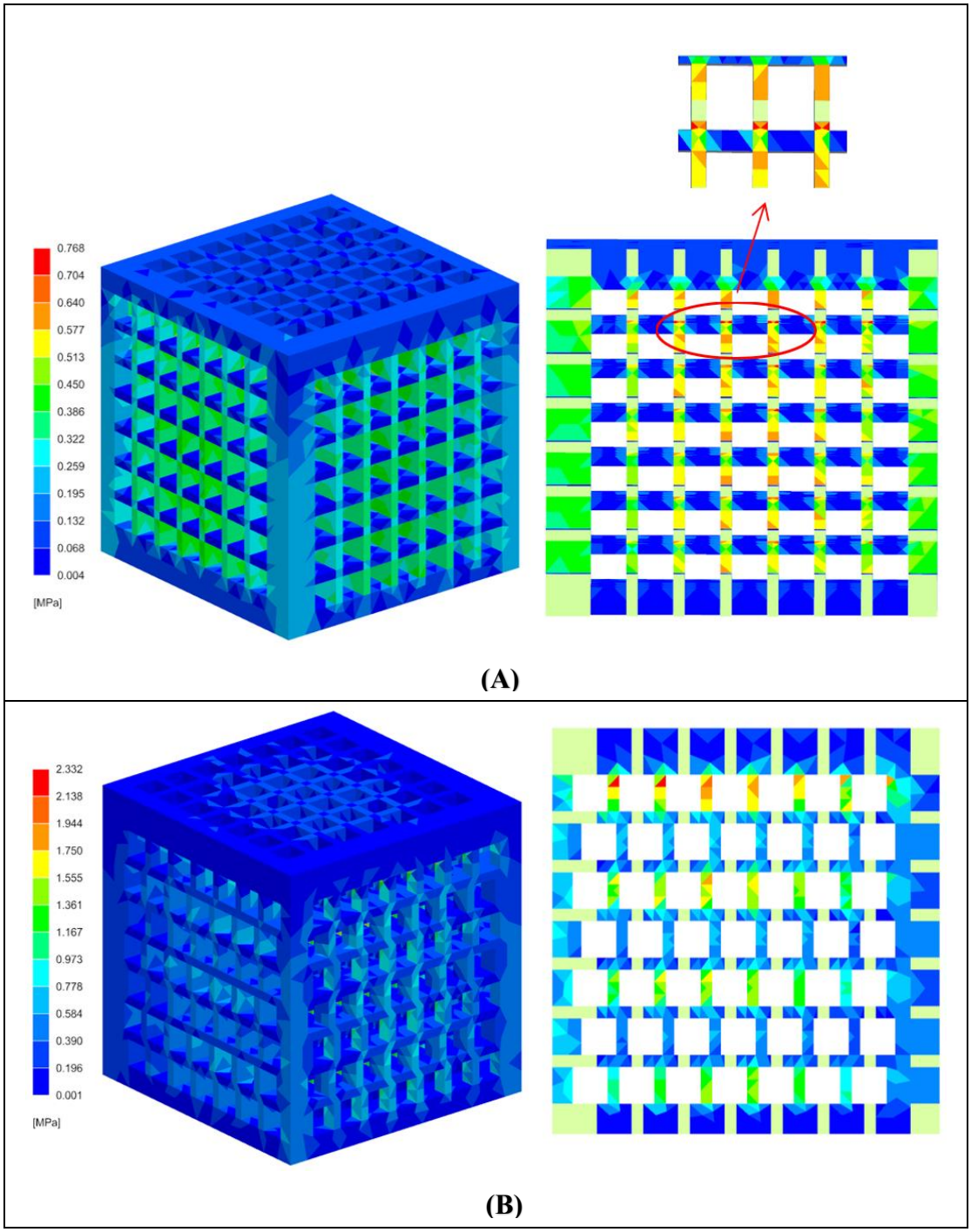

Figure 7: von Mises stress distribution of cubic scaffolding with square hole

Different from the porous cylindrical element scaffold, the von Mises stress distribution of the cubic element scaffold is mainly located inside the scaffold. Figure 7 (A) shows that the scaffold with square holes arranged vertically shows a more uniform stress distribution. The stress of scaffold A is mainly concentrated on the pillars in the same direction as the loading load. The stress on the vertical pillar is minimal and almost 0.

Similar results were obtained for cubical shape scaffold design. In the experimentally validated FEM, showed that the stress distribution has same pattern as the study [29]. In another study, similar results were obtained the stress was high on the porous area of their proposed cubical shape scaffold, while no stress occurs on the diagonals [30]. Its loading capacity is better, and the maximum stress is only 0.768 MPa. The stress distribution of the scaffold with irregularly arranged holes (Figure 7(B)) is concentrated, mainly on the pillars closest to the load application surface.

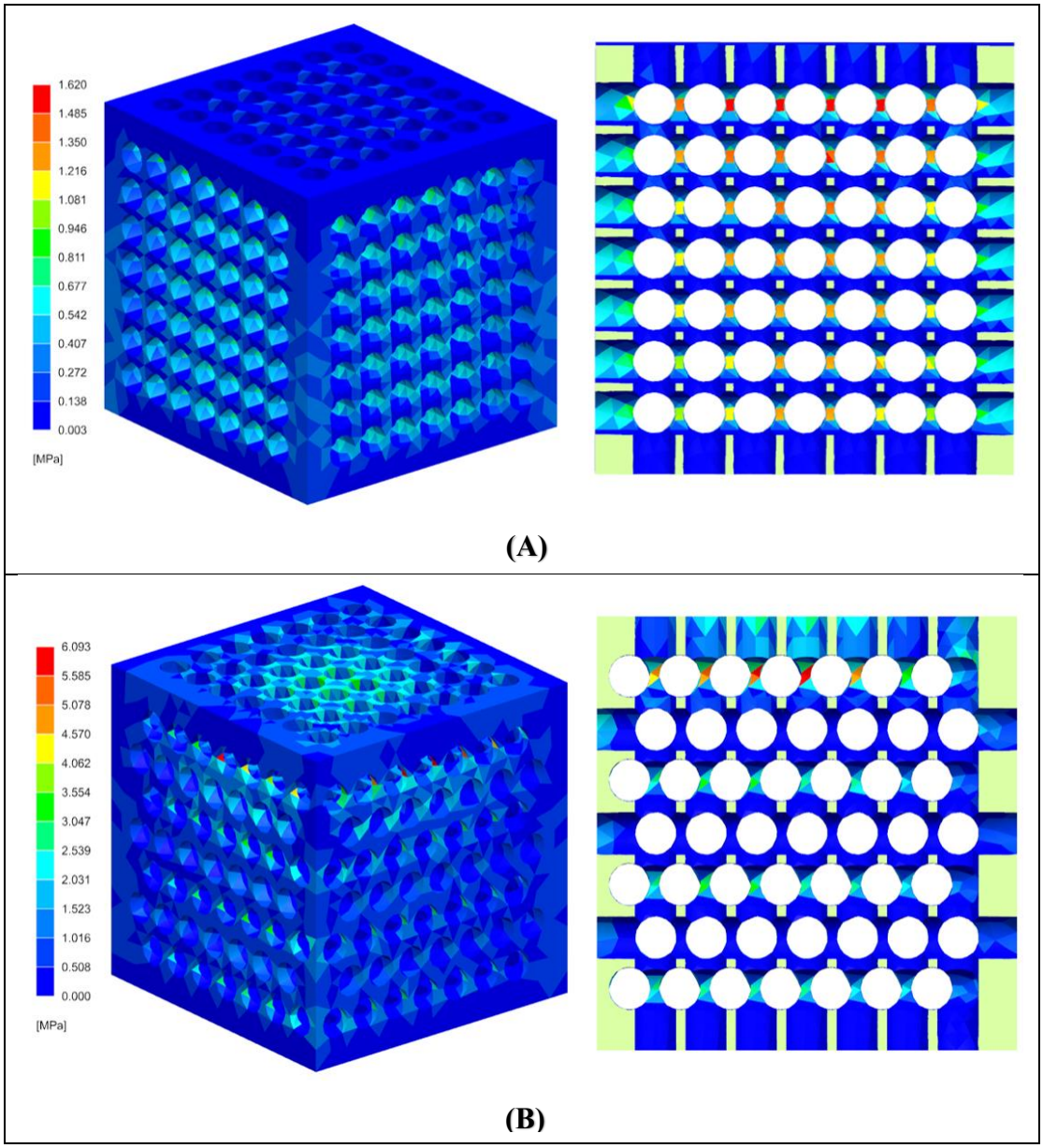

Figure 8: von Mises stress distribution of cubic scaffolding with round holes

The scaffold with round holes Figure 8(A) has a more regular stress distribution, and its stress gradually increases toward the center of the model and the surface where the load is applied. The stress of the staggered round-hole scaffold (Figure 8(B)) is also very concentrated, and it is also distributed on the pillar closest to the loading surface. Still, a small amount of stress distribution can be clearly seen on the loading surface, and its maximum stress distribution is at the center of the circle on the pillar nearby. Among them, the vertical arrangement of square-hole scaffolds in Figure 7 (A) has the smallest maximum stress among the eight designs of scaffolding, which is about 1/93 of that of the scaffolds with staggered round holes in Figure 6 (B). The design with the most massive stress among the cubic scaffolds is the cubic scaffold with staggered round holes. According to Figures 7 and 8, it can be seen that when the holes are arranged in the same way, the scaffold with square holes is less likely to have stress concentration than the round hole scaffold, and its stress distribution is more uniform. Especially in Figure 7(A), the stress is more evenly dispersed inside the scaffold. Such scaffolding has better mechanical performance, and the structure is not easily damaged.

Combined with the above results, it is shown that the staggered arrangement of holes is more likely to cause the stress concentration of the scaffold than the scaffold with a more regular vertical arrangement of holes. The stress of the cylindrical element scaffold in this arrangement is mainly concentrated on the surface where the load is applied, while the stress of the cubic element scaffold is mainly concentrated on the pillar closest to the surface although it is distributed inside the model. Regardless of whether the scaffolds have round holes or square holes, their maximum stress is always higher than that of scaffolds arranged vertically due to the more concentrated stress. And the maximum stress of the round hole cylindrical scaffold (Figure 6 (D) is the largest among these eight models. The shape of the hole will also affect the stent. The loading capacity of a round hole is not as good as that of a square hole, and the maximum stress is concentrated near the loading surface, which is more likely to cause stress concentration.

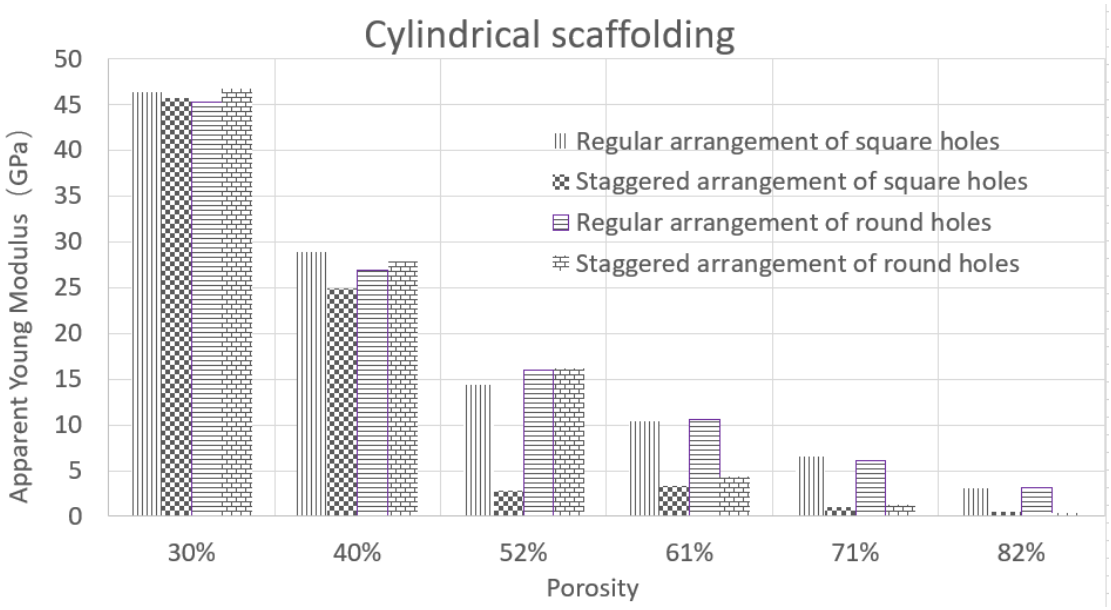

Figure 9: The relationship between the porosity and apparent Young's modulus of cylindrical scaffold

Figures 9 and 10 show the variation of the apparent Young's modulus of the scaffold with porosity. The results show that for these eight models, the apparent Young's modulus decreases as the porosity changes due to the evolution of pore size, and there is a linear behaviour between the porosity and the apparent Young's modulus. It can be seen from Figure 9 that for the cylindrical scaffold, whether the shape of the hole is round or square, the apparent Young's modulus of the two regular porous scaffolds is almost the same under the same porosity. The staggered perforated scaffolding shows different behaviours. When the porosity of the staggered round-hole scaffold is less than or equal to 50%, its apparent Young's modulus is higher than that of the regularly arranged scaffold. This behaviour may be since when the porosity is low, the internal structure of the scaffold is more solid due to the staggered offset. When the porosity is higher than 50%, its apparent Young's modulus is reduced to less than that of scaffolds with regular holes. Regardless of the porosity of the staggered square-hole scaffold, its apparent Young's modulus is smaller than the other three models. And its reduction is relatively significant, with a slight rebound between 50% and 60%, but it is still a downward trend in the end. It can be seen in Figure 9 that the apparent Young's modulus

of the two staggered porous scaffolds is different under low porosity. As the apparent Young's modulus increases, their apparent Young's modulus gradually tends to be consistent. For cylindrical scaffolding, the shape of the hole has little effect on the mechanical properties. Especially after the porosity is higher than 60%, the apparent Young's modulus of scaffolds with the same hole arrangement and different hole types are the same.

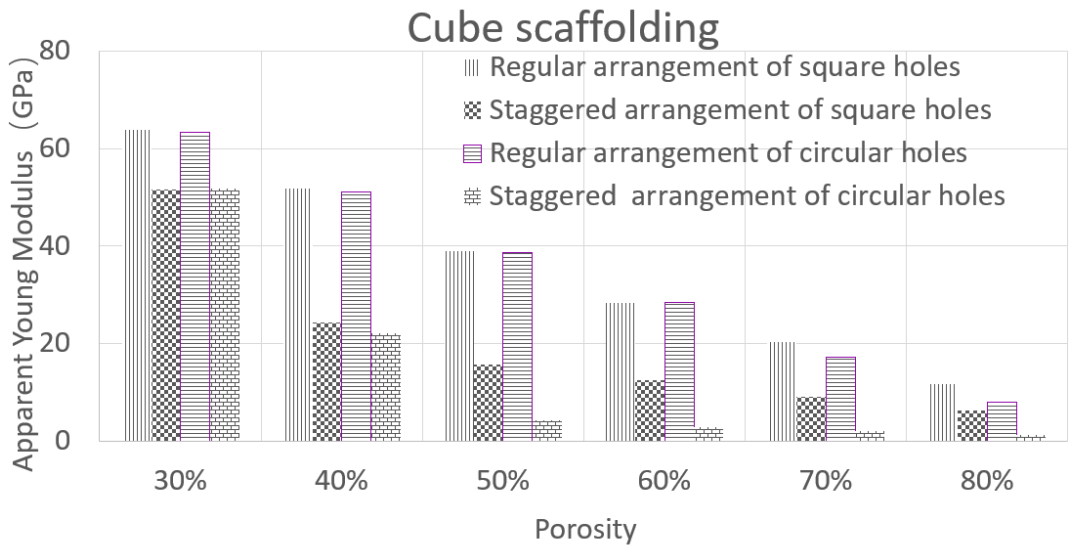

Figure 10: Relationship between the porosity and apparent Young's modulus of cube scaffolding

When the basic shape of the scaffold is a cube (Figure 10), no matter the way of the holes is square or round, the apparent Young's modulus of the scaffold with the staggered porous arrangement is smaller than that of the regularly arranged holes at any porosity. For the scaffold with the regular porous arrangement, when the porosity is less than or equal to 60%, the apparent Young's modulus of the two is almost the same at any porosity. With the increase of porosity, the apparent Young's modulus of the scaffold with square holes under high porosity is more significant than that with round holes. However, the two staggered porous scaffolds exhibit similar behaviour at a low porosity of 30%. When the porosity is higher than 40%, as the porosity increases, the apparent Young's modulus of the round-pored scaffold decreases rapidly, and the apparent Young's modulus apparent Young's of the scaffold has been smaller than the

square hole. Cube scaffolding is different from a cylinder, and the shape of the hole does not affect the scaffold with low porosity. When the porosity is high, the apparent Young's modulus of different hole types is slightly different.

The results show that with the increase of porosity, the apparent Young's modulus of tissue engineering scaffold gradually decreases. The decrease in mechanical properties caused by high porosity will damage the scaffold prematurely, which will limit the choice of tissue scaffold porosity [31]. Regardless of the scaffold design, under the same porosity, the apparent Young's modulus of the scaffolds with two different hole arrangement designs is quite different, and the tissue engineering scaffold with the holes arranged vertically has a better apparent Young's modulus. The mechanical properties of scaffolding are not only affected by porosity, but also by the arrangement of holes.

The apparent Young's modulus of human cortical bone has an extensive elastic range due to the difference in the location of the bone test and the test conditions, and its apparent Young's modulus is between 7.4 and 31.6 GPa [32]. Tissue scaffolding with high porosity can promote the growth and value-added of cells in the body [33]. Scaffolding, as a substitute for damaged tissues or organs, must satisfy the combination of biocompatibility and mechanical properties. Therefore, the main concern here is the mechanical properties of scaffolds with porosity higher than 50%. The regular porous cylindrical scaffold satisfies the apparent Young's modulus range of human cortical bone at a porosity of 50% to 60%, and the apparent Young's modulus of round holes is slightly higher than that of square holes. It is worth noting that the staggered round-hole scaffold also meets the requirements under this porosity. For cubic scaffolds, the apparent Young's modulus of the two regularly arranged scaffolds meets the conditions when the porosity is higher than 60% and less than 80%, and their apparent Young's modulus is larger than that of the cylindrical scaffold with the same porosity. Although the apparent Young's modulus of the staggered square-hole cubic scaffold is not as good as that of the regular arrangement, it also conforms to the apparent Young's modulus range of cortical bone within the porosity range of 50% to 80%. Comparing the above

scaffolding, it can be found that the regularly arranged square-hole cubic scaffolding performs best in all scaffolding designs, that is, it has excellent mechanical properties under high porosity.

4. Conclusions

This study designs eight tissue engineering scaffolds with cubes and cylinders as essential elements, utilizing round and square holes to investigate the effect of pore distribution on mechanical properties through finite element analysis. The research concludes that cylindrical scaffolds with circular holes have a slightly higher apparent Young's modulus within the 30%-50% porosity range. Scaffolds with vertically arranged holes exhibit better loading capacity but are more prone to stress concentration. The apparent Young's modulus of cube-based designs is higher than that of cylinder-based designs at any porosity, and the shape of the hole has little effect on the mechanical properties of the scaffold. The cubic scaffold with a regular porous arrangement performs the best in mimicking the mechanical properties of human cortical bone. Misaligned holes decrease the mechanical properties of scaffolds with the same porosity.

Reference

[1]. Kenkre JS, Bassett JH. The bone remodelling cycle. Annals of clinical biochemistry. 2018 May;55(3):308-27.

[2]. Hollister SJ. Porous scaffold design for tissue engineering. Nature materials. 2005 Jul 1;4(7):518-24.

[3]. O'brien FJ. Biomaterials & scaffolds for tissue engineering. Materials today. 2011 Mar 1;14(3):88-95.

[4]. Niinomi M, Nakai M, Hieda J. Development of new metallic alloys for biomedical applications. Acta biomaterialia. 2012 Nov 1;8(11):3888-903.

[5]. Malladi L, Mahapatro A, Gomes AS. Fabrication of magnesium-based metallic scaffolds for bone tissue engineering. Materials technology. 2018 Jan 28;33(2):173-82.

[6]. Roy S, Panda D, Khutia N, Chowdhury AR. Pore geometry optimization of titanium (Ti6Al4V) alloy, for its application in the fabrication of customized hip implants. International Journal of Biomaterials. 2014 Oct 21;2014.

[7]. Van Noort R. Titanium: the implant material of today. Journal of Materials Science. 1987 Nov; 22:3801-11.

[8] Yu G, Li Z, Li S, Zhang Q, Hua Y, Liu H, Zhao X, Dhaidhai DT, Li W, Wang X. The select of internal architecture for porous Ti alloy scaffold: A compromise between mechanical properties and permeability. Materials & Design. 2020 Jul 1;192:108754.

[9]. Long M, Rack HJ. Titanium alloys in total joint replacement—a materials science perspective. Biomaterials. 1998 Sep 1;19(18):1621-39.

[10]. Xue W, Krishna BV, Bandyopadhyay A, Bose S. Processing and biocompatibility evaluation of laser processed porous titanium. Acta biomaterialia. 2007 Nov 1;3(6):1007-18.

[11]. Li Y, Yang C, Zhao H, Qu S, Li X, Li Y. New developments of Ti-based alloys for biomedical applications. Materials. 2014 Mar 4;7(3):1709-800.

[12]. Sun W, Darling A, Starly B, Nam J. Computer-aided tissue engineering:

overview, scope and challenges. Biotechnology and applied biochemistry. 2004 Feb;39(1):29-47.

[13]. Cansizoglu O, Harrysson OL, Cormier D, West H, Mahale T. Properties of Ti–6Al–4V non-stochastic lattice structures fabricated via electron beam melting. Materials Science and Engineering: A. 2008 Sep 25;492(1-2):468-74.

[14]. Kadkhodapour J, Montazerian H, Raeisi S. Investigating internal architecture effect in plastic deformation and failure for TPMS-based scaffolds using simulation methods and experimental procedure. Materials Science and Engineering: C. 2014 Oct 1;43:587-97.

[15]. Giannitelli SM, Accoto D, Trombetta M, Rainer A. Current trends in the design of scaffolds for computer-aided tissue engineering. Acta biomaterialia. 2014 Feb 1;10(2):580-94.

[16]. Ali D, Sen S. Finite element analysis of mechanical behavior, permeability and fluid induced wall shear stress of high porosity scaffolds with gyroid and lattice-based architectures. Journal of the mechanical behavior of biomedical materials. 2017 Nov 1;75:262-70.

[17]. Filardi V. Stress shielding analysis on easy step staple prosthesis for calcaneus fractures. Journal of Orthopaedics. 2020 Mar 1;18:132-7.

[18] Niinomi M, Nakai M. Titanium-based biomaterials for preventing stress shielding between implant devices and bone. International journal of biomaterials. 2011 Jan 1;2011.

[19]. Ambu R, Morabito AE. Porous scaffold design based on minimal surfaces: Development and assessment of variable architectures. Symmetry. 2018 Aug 25;10(9):361.

[20]. Zhang XY, Fang G, Xing LL, Liu W, Zhou J. Effect of porosity variation strategy on the performance of functionally graded Ti-6Al-4V scaffolds for bone tissue engineering. Materials & Design. 2018 Nov 5;157:523-38.

[21]. Van Grunsven W, Hernandez-Nava E, Reilly GC, Goodall R. Fabrication and mechanical characterisation of titanium lattices with graded porosity. Metals. 2014 Aug 14;4(3):401-9

[22]. Zhou H, Zhao M, Ma Z, Zhang DZ, Fu G. Sheet and network based functionally graded lattice structures manufactured by selective laser melting: Design, mechanical properties, and simulation. International Journal of Mechanical Sciences. 2020 Jun 1; 175:105480

[23]. Nune KC, Kumar A, Misra RD, Li SJ, Hao YL, Yang R. Functional response of osteoblasts in functionally gradient titanium alloy mesh arrays processed by 3D additive manufacturing. Colloids and Surfaces B: Biointerfaces. 2017 Feb 1; 150:78-88.

[24]. Wieding J, Jonitz A, Bader R. The effect of structural design on mechanical properties and cellular response of additive manufactured titanium scaffolds. Materials. 2012 Aug 10;5(8):1336-47

[25]. Pattanayak DK, Fukuda A, Matsushita T, Takemoto M, Fujibayashi S, Sasaki K, Nishida N, Nakamura T, Kokubo T. Bioactive Ti metal analogous to human cancellous bone: Fabrication by selective laser melting and chemical treatments. Acta Biomaterialia. 2011 Mar 1;7(3):1398-406

[26]. Wu S, Liu X, Yeung KW, Liu C, Yang X. Biomimetic porous scaffolds for bone tissue engineering. Materials Science and Engineering: R: Reports. 2014 Jun 1;80:1-36.

[27]. Li S, Zhao S, Hou W, Teng C, Hao Y, Li Y, Yang R, Misra RD. Functionally graded Ti-6Al-4V meshes with high strength and energy absorption. Advanced Engineering Materials. 2016 Jan;18(1):34-8.

[28] Jin H, Zhuo Y, Sun Y, Fu H, Han Z. Microstructure design and degradation performance in vitro of three-dimensional printed bioscaffold for bone tissue engineering. Advances in Mechanical Engineering. 2019 Oct;11(10):1687814019883784.

[29] Shi C, Lu N, Qin Y, Liu M, Li H, Li H. Study on mechanical properties and permeability of elliptical porous scaffold based on the SLM manufactured medical Ti6Al4V. PLoS One. 2021 Mar 4;16(3):e0247764.

[30] Szymczyk P, Hoppe V, Ziółkowski G, Smolnicki M, Madeja M. The effect of geometry on mechanical properties of Ti6Al4V ELI scaffolds manufactured

using additive manufacturing technology. Archives of Civil and Mechanical Engineering. 2020 Mar;20:1-3.

[31]. Karageorgiou V, Kaplan D. Porosity of 3D biomaterial scaffolds and osteogenesis. Biomaterials. 2005 Sep 1;26(27):5474-91.

[32]. Boughton OR, Ma S, Zhao S, Arnold M, Lewis A, Hansen U, Cobb JP, Giuliani F, Abel RL. Measuring bone stiffness using spherical indentation. PLoS One. 2018 Jul 12;13(7):e0200475.

[33]. Gomes ME, Holtorf HL, Reis RL, Mikos AG. Influence of the porosity of starch-based fiber mesh scaffolds on the proliferation and osteogenic differentiation of bone marrow stromal cells cultured in a flow perfusion bioreactor. Tissue engineering. 2006 Apr 1;12(4):801-9.